Vol. 41 (2010) *ACTA PHYSICA POLONICA B* No 5

MEAN FIELD APPROACH AND ROLE OF THE COLOURED NOISE IN THE DYNAMICS OF THREE INTERACTING SPECIES*

Davide Valenti†, Nicola Pizzolato, Bernardo Spagnolo

Dipartimento di Fisica e Tecnologie Relative, Group of Interdisciplinary Physics‡
Università di Palermo and CNISM-INFM, Unità di Palermo
Viale delle Scienze, edificio 18, I-90128 Palermo, Italy

(Received February 2, 2010)

We study the effects of the coloured noise on the dynamics of three interacting species, namely two preys and one predator, in a two-dimensional lattice with N sites. The three species are affected by multiplicative time correlated noise, which accounts for the effects of environment on the species evolution. Moreover, the interaction parameter between the two preys is a dichotomous stochastic process, which determines two dynamical regimes corresponding to different biological conditions. Preliminarily, we study the noise effect on the three species dynamics in single site. Then, we use a mean field approach to obtain, in Gaussian approximation, the moment equations for the species densities. We find that the multiplicative noise does not affect the time behaviour of the 1st order moments. Conversely, the 2nd order moments are strongly dependent both on the intensity and correlation time of the multiplicative noise. Finally, we compare our results with those obtained from a discrete time approach based on a model of coupled map lattice.

PACS numbers: 05.40.–a, 02.50.–r, 87.23.Cc, 05.45.Ra

1. Introduction

It is known that noise can play a constructive role in nonlinear systems, and counterintuitive effects such as stochastic resonance [1–3], noise enhanced stability [4] and noise delayed extinction [5, 6] can appear in biological systems, whose dynamics is governed by nonlinear interactions and

---

[*] Presented at the XXII Marian Smoluchowski Symposium on Statistical Physics, Zakopane, Poland, September 12–17, 2009.

[†] `valentid@gip.dft.unipa.it`

[‡] `http://gip.dft.unipa.it`

noisy perturbations [7]. Noise can be the key to analyze phenomena that are difficult to explain in a fully deterministic regime, such as fluctuations of biological species in natural ecosystems [8–11], bacterial growth in food products and role of molecular noise in the time behavior of a single bacterium [12], dynamics of disease connected with genetic mutations [13], genotypic, phenotypic and behavioural diversity [14–17]. In these systems and more generally in biology and ecology, random fluctuations of temperature, natural resources and other environmental parameters can be modeled by sources of multiplicative noise [6, 18–22].

In particular, spatio-temporal behaviour and formation of spatial patterns have recently attracted the interest of scientists in different research fields, ranging from hydrodynamics systems, nonlinear optics, oscillatory chemical reactions and excitable biological media [23], to nonlinear models for interacting populations [24], two-dimensional prey-predator systems [25–27] and reaction-diffusion systems with pattern formation [28]. During the last three decades an approach exploiting moments has been widely used to analyse the spatio-temporal dynamics of different species [29, 30], quantum systems in the context of nonlinear Schrödinger equations [31], and kinetic models of polymer dynamics [32].

In this paper we study the spatio-temporal behaviour of three interacting species, *i.e.* two preys and one predator, subjected to random fluctuations. The system is described by generalized Lotka–Volterra equations [33, 34] in the presence of two noise sources: *(i)* a time correlated multiplicative noise, modeled as an Ornstein–Uhlenbeck process [35], which accounts for the effects of environment fluctuations on the biological species; *(ii)* a noisy interaction parameter which is a stochastic process, whose dynamics is given by a periodic function in the presence of a correlated dichotomous noise. We define a two-dimensional spatial domain considering in each site a system of three Lotka–Volterra equations coupled by interaction terms [36]. Afterwards, using a mean field approach, we study the dynamics of the system by the moment equations within the Gaussian approximation [37–39], obtaining the time behaviour of the 1st and 2nd order moments for the three species concentrations. Finally, we analyse the system dynamics by using a coupled map lattice model [40], and compare the results with those obtained within the formalism of the moments.

2. The model

Our system is described by generalized Lotka–Volterra equations, within the Ito scheme [35], with diffusive terms in a two-dimensional lattice with N sites:

$$\begin{aligned}
\dot{x}_{i,j} &= \lambda x_{i,j}(1-\nu x_{i,j}-\beta y_{i,j}-\alpha z_{i,j})+x_{i,j}\zeta^x_{i,j}+D(\langle x\rangle - x_{i,j})\,, \quad (1)\\
\dot{y}_{i,j} &= \lambda y_{i,j}(1-\nu y_{i,j}-\beta x_{i,j}-\alpha z_{i,j})+y_{i,j}\zeta^y_{i,j}+D(\langle y\rangle - y_{i,j})\,, \quad (2)\\
\dot{z}_{i,j} &= \lambda_z z_{i,j}[-1+\gamma(x_{i,j}+y_{i,j})]+z_{i,j}\zeta^z_{i,j}+D(\langle z\rangle - z_{i,j})\,, \quad (3)
\end{aligned}$$

where the dot indicates the time derivative. The variables $x_{i,j}$, $y_{i,j}$ and $z_{i,j}$ are functions of the time t, and denote the densities of the two preys and predator, respectively, in the lattice site (i,j). λ and λ_z are scale factors, ν is the saturation parameter for the two preys, D is the diffusion coefficient, and $\langle x\rangle$, $\langle y\rangle$, $\langle z\rangle$ indicate the spatial mean, performed on the whole lattice, of the three species densities. The coefficient β is the interaction parameter between the two preys. The coefficients α and γ account for the interaction between preys and predator. $\zeta^l_{i,j}(t)$ $(l=x,y,z)$ are statistically independent coloured noises that model the interaction between species and environment. The coloured noises are exponentially correlated sources given by the Ornstein–Uhlenbeck process [35]

$$\frac{d\zeta^l_{i,j}}{dt} = -\frac{1}{\tau^l_c}\,\zeta^l_{i,j}+\frac{1}{\tau^l_c}\,\xi^l_{i,j}(t)\,, \qquad (l=x,y,z) \tag{4}$$

and $\xi^l_{i,j}(t)$ $(l=x,y,z)$ are statistically independent Gaussian white noises, within the Ito scheme, with zero mean and correlation function $\langle\xi^l_{i,j}(t)\xi^{l'}_{i',j'}(t')\rangle = \sigma^l\delta(t-t')\delta_{ll'}\delta_{ii'}\delta_{jj'}$. The correlation function of the processes of Eq. (4) is

$$\left\langle \zeta^l_{i,j}(t)\zeta^{l'}_{i',j'}(t')\right\rangle = \frac{\sigma^l}{2\tau^l_c}\;e^{-|t-t'|/\tau^l_c}\,\delta_{ll'}\delta_{ii'}\delta_{jj'} \tag{5}$$

and gives $\sigma^l\delta(t-t')\delta_{ll'}\delta_{ii'}\delta_{jj'}$ in the limit $\tau^l_c\to 0$.

2.1. Single site dynamics

2.1.1. Stationary states and dynamical regimes

Depending on the value of the interaction parameter, coexistence or exclusion regime takes place. In the absence of diffusion terms ($D=0$), Eqs. (1)–(3) become

$$\begin{aligned}
\dot{x} &= \lambda x(1-\nu x-\beta y-\alpha z)+x\zeta^x\,, \quad (6)\\
\dot{y} &= \lambda y(1-\nu y-\beta x-\alpha z)+y\zeta^y\,, \quad (7)\\
\dot{z} &= \lambda_z z\,[-1+\gamma(x+y)]+z_{i,j}\zeta^z\,, \quad (8)
\end{aligned}$$

where the indices i,j were suppressed. Eqs. (6)–(8) describe the dynamics of a single site ecosystem. In these conditions, setting at zero the multiplicative noise ($\zeta^x(0) = \zeta^y(0) = \zeta^z(0) = 0$, $\sigma^x = \sigma^y = \sigma^z = 0$), for the generic site of lattice the stationary values of the three species densities are given by

$$x^{\text{stat}} = y^{\text{stat}} = \frac{1}{2\gamma}\,, \tag{9}$$

$$z^{\text{stat}} = \frac{2\gamma - (\beta + \nu)}{2\alpha\gamma}\,. \tag{10}$$

From Eq. (9) one can see that the two prey densities have stationary values that are independent of the interaction parameter β. Conversely, the stationary value of the predator density (Eq. (10)) is connected with the value of β. This indicates that the interaction parameter between the two preys determines the coexistence or exclusion regime for the whole system through the stationary value z^{stat}. From Eq. (10) the survival condition for the predator is $z^{\text{stat}} > 0$, which allows to get the coexistence condition for the three species as a function of β

$$\beta < 2\gamma - \nu\,. \tag{11}$$

The inequality (11) indicates that the system is characterized by two stationary states, which become stable or unstable depending on the values that β, γ and ν take on.

In order to determine the conditions for which the stationary values given in Eqs. (9), (10) correspond to a point of stable equilibrium in the phase space, we perform a stability analysis for the deterministic dynamics in single site. Therefore, in Eqs. (6)–(8) we neglect the noise terms and consider the generic site of lattice. Afterwards, we obtain the equations for the variations δx, δy, δz around the stationary values x^{stat}, y^{stat}, z^{stat}. This is a linear system of three algebraic equations that can be easily solved [39], finding the expressions for the eigenvalues and corresponding eigenvectors. Obviously, the stability of the equilibrium point given by Eqs. (9), (10) depends on the values of the system parameters. Setting $\lambda = 3$, $\lambda_z = 0.06$, $\nu = 1$, $\alpha = 0.02$, $\gamma = 1$, we calculate the eigenvalues and eigenvectors for two different values of the interaction parameter β, *i.e.* $\beta = \beta_{\text{down}} = 0.94$ and $\beta = \beta_{\text{up}} = 1.04$, corresponding to coexistence and exclusion regime, respectively. The results reported in Ref. [39] show that the equilibrium point given by Eqs. (9), (10) is stable for $\beta = \beta_{\text{down}}$ and unstable for $\beta = \beta_{\text{up}}$. Finally, setting $D = 0$, we calculate the numerical solution for single site dynamics by integrating Eqs. (6)–(8), using $\beta = \beta_{\text{down}}$ and $\beta = \beta_{\text{up}}$ and the same parameter values as in the stability analysis. Here, initial conditions, intensities and correlation times of the multiplicative noise sources are the same for the three species, that is $\zeta(0) = \zeta^x(0) = \zeta^y(0) = \zeta^z(0)$, $\sigma = \sigma^x = \sigma^y = \sigma^z$, $\tau_{\text{c}} = \tau_c^x = \tau_c^y = \tau_c^z$. The initial conditions for the species are $x(0) = y(0) = 0.1$, $z(0) = 2.0$.

According to the stability analysis, the results obtained (see Fig. 1) in the absence of noise ($\zeta(0) = 0$, $\sigma = 0$) and under the influence of white noise ($\zeta(0) = 0$, $\sigma = 10^{-16}$, $\tau_c = 0$) indicate clearly that the system is stable for $\beta = \beta_{\mathrm{down}}$ and unstable for $\beta = \beta_{\mathrm{up}}$ (see discussion in Ref. [39]). In panels (a), (b) and (c) of Fig. 1, the densities of the two preys overlap and the time series of species x (blue line) is not visible.

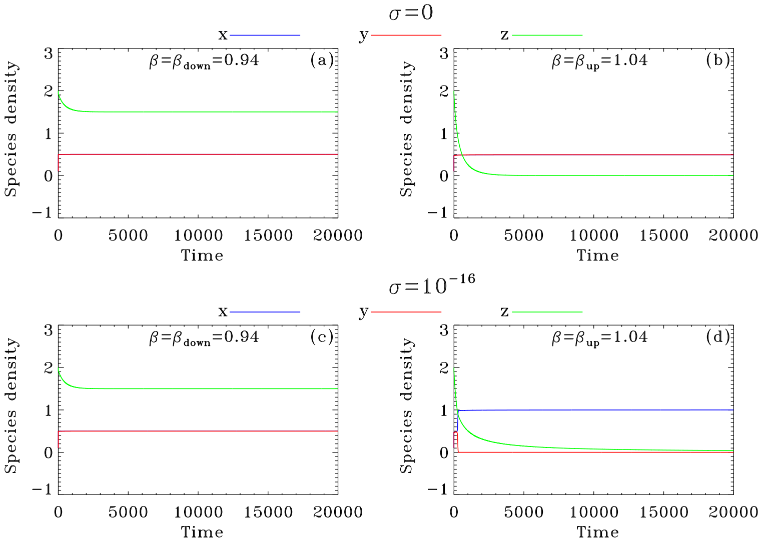

Fig. 1. Time evolution of the three species. Deterministic dynamics in (a) coexistence and (b) exclusion regime. Stochastic dynamics, for $\zeta(0) = 0$, $\sigma = 10^{-16}$ in (c) coexistence and (d) exclusion regime. In panels (a), (b) and (c), the densities of the two preys overlap maintaining the constant value 0.5 and the time series of species x (blue line) are not visible. In panel (d) prey x maintains the constant value 1.0, while prey y disappears after few time steps. Values of the parameters and initial conditions are $\lambda = 3$, $\lambda_z = 0.06$, $\nu = 1$, $\alpha = 0.02$, $\gamma = 1$, $x(0) = y(0) = 0.1$, $z(0) = 2.0$.

2.2. *The interaction parameter*

The value of the interaction parameter β is crucial for the dynamical regime of the ecosystem investigated. In fact, for $\beta < 1$ both species survive and a coexistence regime takes place, while for $\beta > 1$ at least one of the species extinguishes after a certain time, and exclusion occurs. These two regimes correspond to stable states of the Lotka–Volterra's deterministic model [39]. From a biological point of view it is reasonable to consider that, in a real ecosystem, environmental and climatic variables, such as temperature, can be subjected to periodical and random forces, which modify the dynamics of the biological species, driving the system alternatively between the coexistence ($\beta < 1$) and exclusion ($\beta > 1$) regimes. To describe this dynamical behaviour we consider, as interaction parameter $\beta(t)$, a dichotomous stochastic process, whose jump rate is a periodic function with period $T = (2\pi)/\omega$

$$\chi(t) = \begin{cases} 0\,, & \Delta t \leq \tau_{\mathrm{d}}\,, \\ \chi_0\,(1 + A\,|\cos\omega t|)\,, & \Delta t > \tau_{\mathrm{d}}\,. \end{cases} \tag{12}$$

Here Δt is the time interval between two consecutive switches, and τ_{d} is the delay between two jumps, that is the time interval after a switch, before another jump can occur. In Eq. (12), A and ω are amplitude and angular frequency, respectively, of the periodic term, and χ_0 is the jump rate in the absence of periodic term. Setting $\beta_{\mathrm{down}} = 0.94 < 1$ and $\beta_{\mathrm{up}} = 1.04 > 1$, the dichotomous noise causes the system to jump between coexistence and exclusion regime. For $\tau_{\mathrm{d}} = 435$ this behaviour becomes quasi-periodical. In these conditions, a competition regime is established with the system switching quasi-periodically from coexistence to exclusion regime [6] (see Fig. 2 and discussion in Ref. [30]). This synchronization effect can be considered as a signature of the stochastic resonance phenomenon [1].

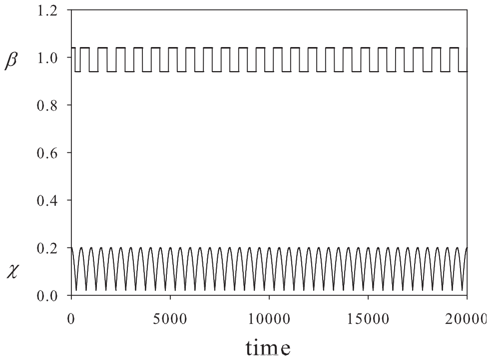

Fig. 2. Time evolution of the interaction parameter $\beta(t)$ with initial value $\beta(0) = 1.04$ and delay time $\tau_{\mathrm{d}} = 435$. The interaction parameter $\beta(t)$ switches quasi-periodically between $\beta_{\mathrm{down}} = 0.94$ and $\beta_{\mathrm{up}} = 1.04$. The values of the other parameters are $A = 9.0$, $\omega/(2\pi) = 10^{-3}$, $\chi_0 = 2 \times 10^{-2}$.

2.2.1. Time behaviour of the species in a single site

In this section we analyse the time behaviour of the three interacting species in a single site of the lattice in the presence of coloured noise. Setting $\sigma = \sigma^x = \sigma^y = \sigma^z$ and $\tau_{\mathrm{c}} = \tau_c^x = \tau_c^y = \tau_c^z$, we get three statistically independent Ornstein–Uhlenbeck processes $\zeta^x(t)$, $\zeta^y(t)$, $\zeta^z(t)$ with the same intensity and correlation time. By choosing $\beta(0) = 1.04$ and $\tau_{\rm d} = 435$, we obtain for $\beta(t)$ the time behaviour shown in Fig. 2. By numerically solving Eqs. (6)–(8), we calculate the time series of x, y and z for two different values of the multiplicative noise intensity, namely $\sigma = 10^{-6}, 10^{-3}$, and three values of correlation time, *i.e.* $\tau_{\rm c} = 0$ (white noise), $100, 1000$. The values of the other parameters are the same used in the previous section, that is $\lambda = 3$, $\lambda_z = 0.06$, $\nu = 1$, $\alpha = 0.02$, $\gamma = 1$, $\beta_{\rm down} = 0.94$, $\beta_{\rm up} = 1.04$. The initial values of the species densities are $x(0) = y(0) = 0.1$, $z(0) = 2.0$. Here and throughout the paper, the initial values of the Ornstein–Uhlenbeck processes are $\zeta^x(0) = \zeta^y(0) = \zeta^z(0) = 0$. The time series for $\sigma = 10^{-6}$ are shown in Fig. 3 (a), (b), (c). Here, an anticorrelated oscillating behaviour of $x(t)$ and $y(t)$ (preys) appears for white noise (panel a), with the two prey densities oscillating, around the stationary values $x^{\rm stat} = y^{\rm stat} = 0.5$, at the same frequency of the external driving force. We observe that the predator density also shows an oscillating behaviour, with the same frequency, around a value much smaller than $z^{\rm stat} = 1.5$, because of the dependence of $z^{\rm stat}$ on the parameter β. However, the oscillations of $z(t)$ are characterized by a smaller amplitude with respect to $x(t)$ and $y(t)$. For $\sigma = 10^{-6}$ no difference appears in the presence of coloured noise with respect to the case of white noise (compare in Fig. 3 panel (a) with panels (b), (c)).

A different behaviour is observed for $\sigma = 10^{-3}$: in this case the role played by the coloured noise becomes visible (compare in Fig. 3 panel (d) with panels (e), (f)). In particular, a reduction of the noise effects is observed as the correlation time increases: the predator disappears in the presence of white noise (see panel (d)), while survives under the action of coloured noise (see panels (e), (f)).

2.3. Spatially extended system: mean field approach

In this section we analyse the time behaviour of three interacting species in a spatially extended system by using a mean field approach. The system dynamics is described by Eqs. (1)–(3) in the presence of diffusive terms ($D \neq 0$). In order to use a mean field approach we derive the moment equations for this system. Assuming $N \to \infty$, we write Eqs. (1)–(3) in a mean field form

$$\begin{aligned} \dot{x} &= f_x(x,y,z) + g_x(x)\zeta^x(t) + D(\langle x\rangle - x)\,, &(13)\\ \dot{y} &= f_y(x,y,z) + g_y(y)\zeta^y(t) + D(\langle y\rangle - y)\,, &(14)\\ \dot{z} &= f_z(x,y,z) + g_z(y)\zeta^z(t) + D(\langle z\rangle - z)\,, &(15)\end{aligned}$$

where $\langle x\rangle$, $\langle y\rangle$ and $\langle z\rangle$ are average values on the spatial lattice considered (ensemble averages in the thermodynamic limit) and we set $f_x(x,y,z) = \lambda x(1 - \nu x - \beta y - \alpha z)$, $g_x(x) = x$, $f_y(x,y,z) = \lambda y(1 - \nu y - \beta x - \alpha z)$,

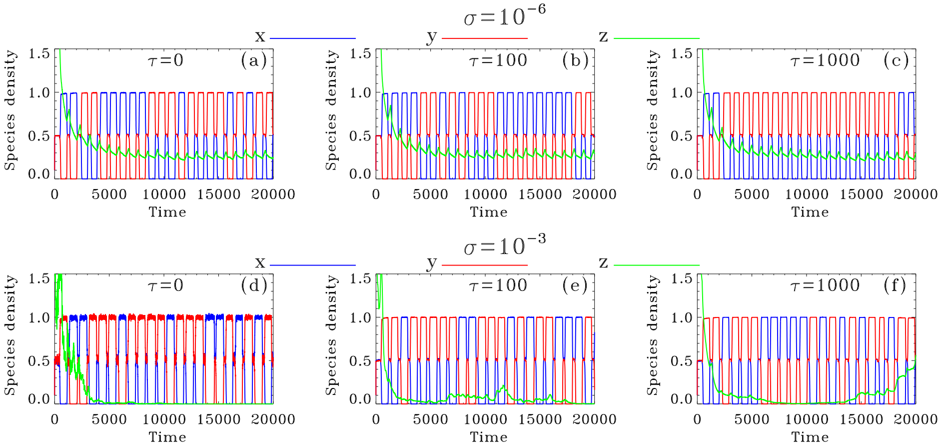

Fig. 3. Time evolution of the three species densities in a single site of the lattice for two different values of the multiplicative noise intensity ($\sigma = 10^{-6}, 10^{-3}$). The values of the correlation time are: $\tau_c = 0$ (white noise), 100, 1000. Here $\lambda = 3$, $\lambda_z = 0.06$, $\nu = 1$, $\alpha = 0.02$, $\gamma = 1$. The values of the other parameters are the same as of Fig. 2. The initial values are $x(0)=y(0) = 0.1$, $z(0)=2.0$, and $\zeta(0)=0$. In all panels the two preys (x and y) show anticorrelated oscillations around 0.5. For $\sigma = 10^{-3}$ different behaviour appears due to the coloured noise: the time correlation (see panels (e), (f)) tends to reduce the effects observed in the presence of white noise (see panels (a), (d)), allowing the predator to survive also in the presence of higher noise intensities.

$g_y(y) = y$, $f_z(x,y,z) = \lambda_z z[-1 + \gamma(x + y)]$, $g_z(z) = z$. By site averaging Eqs. (13)–(15), we obtain

$$\begin{aligned}\langle\dot{x}\rangle &= \langle f_x(x,y,z)\rangle\,,\\ \langle\dot{y}\rangle &= \langle f_y(x,y,z)\rangle\,,\\ \langle\dot{z}\rangle &= \langle f_z(x,y,z)\rangle\,. \qquad (16)\end{aligned}$$

By expanding the functions $f_x(x,y,z)$, $g_x(x)$, $f_y(x,y,z)$, $g_y(y)$, $f_z(x,y,z)$, $g_z(z)$ around the 1st order moments $\langle x(t)\rangle$, $\langle y(t)\rangle$ and $\langle z(t)\rangle$, we get an infinite set of simultaneous ordinary differential equations for all the moments [37]. To truncate this set we apply a Gaussian approximation, for which the cumulants above the 2nd order vanish. Therefore we obtain

$$\langle\dot{x}\rangle = \lambda\langle x\rangle(1 - \nu\langle x\rangle - \beta\langle y\rangle - \alpha\langle z\rangle) - \lambda(\nu\mu_{200} + \beta\mu_{110} + \alpha\mu_{101})\,, \qquad (17)$$

$$\langle\dot{y}\rangle = \lambda\langle y\rangle(1 - \nu\langle y\rangle - \beta\langle x\rangle - \alpha\langle z\rangle) - \lambda(\nu\mu_{020} + \beta\mu_{110} + \alpha\mu_{011})\,, \qquad (18)$$

$$\langle\dot{z}\rangle = \lambda_z\langle z\rangle(-1 + \gamma\langle x\rangle + \gamma\langle y\rangle) + \lambda_z\gamma(\mu_{101} + \mu_{011})\,, \qquad (19)$$

$$\begin{aligned}
\dot{\mu}_{200} &= 2\lambda(1-2\nu\langle x\rangle-\beta\langle y\rangle-\alpha\langle z\rangle)\mu_{200}-2\lambda\langle x\rangle(\beta\mu_{110}+\alpha\mu_{101}) \\
&\quad +2\sigma_x(\mu_{200}+\langle x\rangle^2)(1-e^{-t/\tau_x^c})-2D\mu_{200}\,, \qquad (20)\\
\dot{\mu}_{020} &= 2\lambda(1-2\nu\langle y\rangle-\beta\langle x\rangle-\alpha\langle z\rangle)\mu_{020}-2\lambda\langle y\rangle(\beta\mu_{110}+\alpha\mu_{011}) \\
&\quad +2\sigma_y(\mu_{020}+\langle y\rangle^2)(1-e^{-t/\tau_y^c})-2D\mu_{020}\,, \qquad (21)\\
\dot{\mu}_{002} &= 2\lambda_z(-1+\gamma\langle x\rangle+\gamma\langle y\rangle)\mu_{002}+2\lambda_z\gamma\langle z\rangle(\mu_{101}+\mu_{011}) \\
&\quad +2\sigma_z(\mu_{002}+\langle z\rangle^2)(1-e^{-t/\tau_z^c})-2D\mu_{002}\,, \qquad (22)\\
\dot{\mu}_{110} &= \lambda[2-(2\nu+\beta)(\langle x\rangle+\langle y\rangle)-2\alpha\langle z\rangle]\mu_{110}-\lambda\beta(\langle x\rangle\mu_{020}+\langle y\rangle\mu_{200}) \\
&\quad -\lambda\alpha(\langle x\rangle\mu_{011}+\langle y\rangle\mu_{101})-2D\mu_{110}\,, \qquad (23)\\
\dot{\mu}_{101} &= \lambda(1-2\nu\langle x\rangle-\beta\langle y\rangle-\alpha\langle z\rangle)\mu_{101}+\lambda_z(-1+\gamma\langle x\rangle+\gamma\langle y\rangle)\mu_{101} \\
&\quad -\lambda\langle x\rangle(\alpha\mu_{002}+\beta\mu_{011})+\lambda_z\gamma\langle z\rangle(\mu_{110}+\mu_{200})-2D\mu_{101}\,, \qquad (24)\\
\dot{\mu}_{011} &= \lambda(1-2\nu\langle y\rangle-\beta\langle x\rangle-\alpha\langle z\rangle)\mu_{011}+\lambda_z(-1+\gamma\langle x\rangle+\gamma\langle y\rangle)\mu_{011} \\
&\quad -\lambda\langle y\rangle(\alpha\mu_{002}+\beta\mu_{101})+\lambda_z\gamma\langle z\rangle(\mu_{110}+\mu_{020})-2D\mu_{011}\,, \qquad (25)
\end{aligned}$$

where μ_{200}, μ_{020}, μ_{002}, μ_{110}, μ_{101}, μ_{011} are the 2nd order central moments defined on the lattice

$$\begin{aligned}
\mu_{200}(t) &= \langle x^2\rangle-\langle x\rangle^2\,, &\quad \mu_{110}(t)&=\langle xy\rangle-\langle x\rangle\langle y\rangle,\\
\mu_{020}(t) &= \langle y^2\rangle-\langle y\rangle^2\,, &\quad \mu_{101}(t)&=\langle xz\rangle-\langle x\rangle\langle z\rangle,\\
\mu_{002}(t) &= \langle z^2\rangle-\langle z\rangle^2\,, &\quad \mu_{011}(t)&=\langle yz\rangle-\langle y\rangle\langle z\rangle\,. \qquad (26)
\end{aligned}$$

In order to get the dynamics of the three species, we analyse the time evolution of the 1st and 2nd order moments according to Eqs. (17)–(25). As initial conditions we consider each species uniformly distributed on the spatial domain, setting $\langle x(0)\rangle = \langle y(0)\rangle = 0.1$, $\langle z(0)\rangle = 2.0$, $\mu_{200}(0) = \mu_{020}(0) = \mu_{002}(0) = \mu_{110}(0) = \mu_{101}(0) = \mu_{011}(0) = 0$. Afterwards, from Eqs. (17)–(25) we obtain, in the deterministic case, the stationary values for $\langle x\rangle$, $\langle y\rangle$ and $\langle z\rangle$

$$\langle x\rangle^{\rm stat}=\langle y\rangle^{\rm stat}=\frac{1}{2\gamma}\,,\qquad \langle z\rangle^{\rm stat}=\frac{2\gamma-(\beta_{\rm down}+\nu)}{2\alpha\gamma}\,. \qquad (27)$$

Using for the parameters the same values as in the single site analysis, we find

$$\langle x\rangle^{\rm stat}=\langle y\rangle^{\rm stat}=0.5\,,\qquad \langle z\rangle^{\rm stat}=1.5\,. \qquad (28)$$

Finally, using for the diffusion constant $D = 10^{-1}$, and setting the delay time at the same value, $\tau_{\rm d} = 435$, used in the single site analysis, by numerical integration of Eqs. (17)–(25), we calculate the time series of the 1st and 2nd order moments for the same values of multiplicative noise intensity

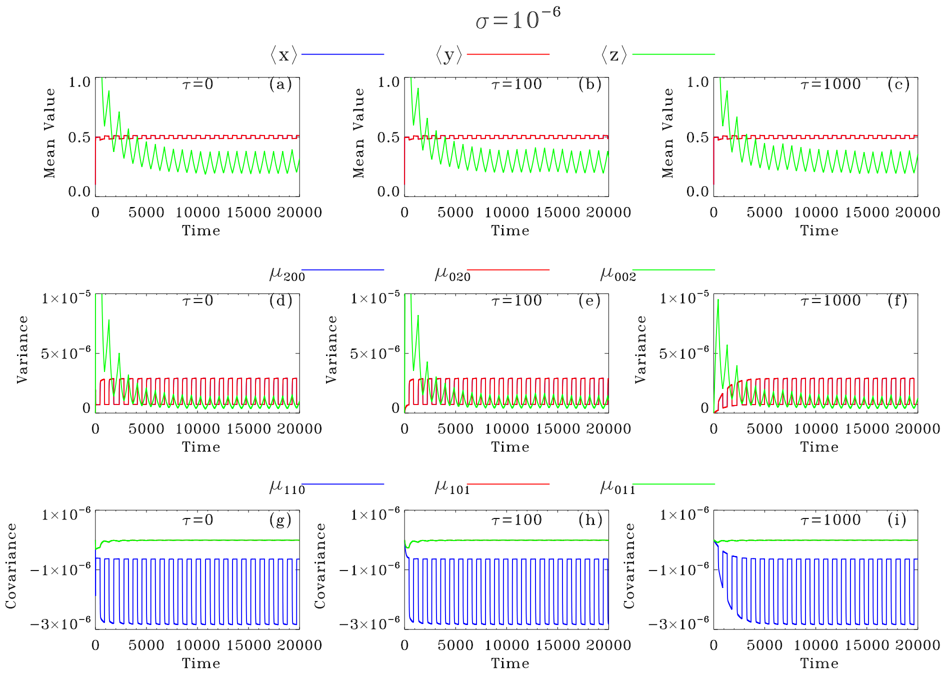

Fig. 4. Time evolution of the 1st and 2nd order moments in the mean field approach, for $\sigma = 10^{-6}$ and three values of correlation time, $\tau_c = 0$ (white noise), $100, 1000$. The mean value of the predator, $\langle z(t)\rangle$, shows a behaviour correlated with those of both preys, $\langle x(t)\rangle$ and $\langle y(t)\rangle$, that are completely overlapped oscillating around 0.5 (panels (a)–(c)). In panels (d)–(f) the moments μ_{200} and μ_{020} are completely overlapped and oscillate between 0 and 2.5×10^{-6}. Replacing white noise with coloured one affects the 2nd order moments, introducing a delay: the maximum amplitude of the oscillations in the time series of the 2nd order moments is reached after a time interval that increases as τ_c becomes larger. In panels (a)–(f), the time series of mean values and variances of the two prey densities overlap and those of species x (blue line) are not visible. In panels (g)–(i), the covariances μ_{101} and μ_{011} overlap at the constant value 0, being μ_{101} (red line) not visible. The initial values are $\langle x(0)\rangle = \langle y(0)\rangle = 0.1$, $\langle z(0)\rangle = 2.0$, $\mu_{200}(0) = \mu_{020}(0) = \mu_{002}(0) = \mu_{110}(0) = \mu_{101}(0) = 0 = \mu_{011}(0) = 0$, and $\zeta(0) = 0$. The diffusion coefficient is $D = 10^{-1}$. The values of the other parameters are the same used in Fig. 3.

and correlation time used in the single site analysis. The results are shown in Figs. 4, 5. Here we note that, after a transient, the mean values of the two prey densities (see panels (a), (b), (c) of Figs. 4, 5) oscillate around the stationary values $\langle x\rangle^{\mathrm{stat}}$, $\langle y\rangle^{\mathrm{stat}}$, while the predator shows a periodical behavior around a value much smaller than $\langle z\rangle^{\mathrm{stat}}$ (see Eqs. (28)). Different

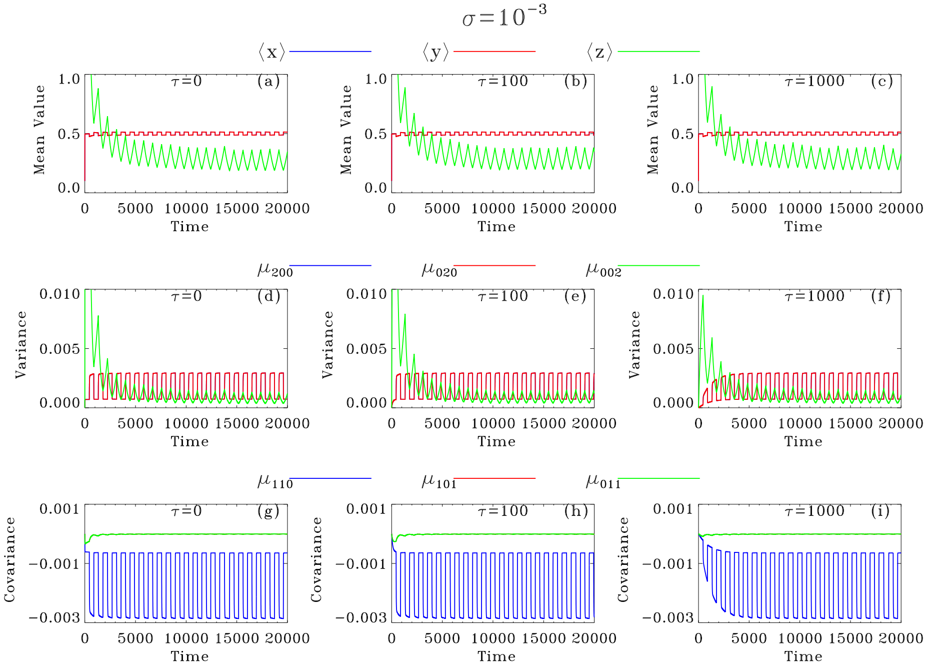

Fig. 5. Time evolution of the 1st and 2nd order moments in the mean field approach, for $\sigma = 10^{-3}$ and three values of correlation time, $\tau_c = 0$ (white noise), 100, 1000. The time series of the mean values (panels a, b, c) are identical to those shown in panels (a), (b), (c) of Fig. 4. However, the larger value of noise intensity ($\sigma = 10^{-3}$) affects the 2nd order moments, causing the amplitude of the oscillations to be enhanced (compare panels (d)–(i), with the same panels in Fig. 4). The oscillations reach the maximum amplitude after a time interval that increases as τ_c becomes larger. In panels (a)–(f), the time series of mean values and variances of the two prey densities overlap and those of species x (blue line) are not visible. In panels (g)–(i), the covariances μ_{101} and μ_{011} overlap, being μ_{101} (red line) not visible. The initial conditions and parameter values are the same as in Fig. 4.

intensities of the multiplicative noise do not produce any changes in the behaviour of the mean values (see panels (a), (b), (c) of Figs. 4, 5). Conversely, the amplitude of the oscillations of the 2nd order moments is enhanced as the noise intensity increases and scales with the order of magnitude of σ. As a consequence we observe an enhancement of: *(i)* anticorrelated behaviour between the two preys; *(ii)* uncorrelated behaviour between the predator and each prey; *(iii)* correlated behaviour between the predator and the total prey density (a global increase of food availability improves the life conditions of the predator). This dependence of the 2nd order moments on the noise intensity is not strange. In fact, the 2nd order moments account for the spatial dispersion of the species. Therefore, as one can expects, higher values of the noise intensity cause the species densities to spread out in the lattice.

In the present work we intend to study the role of the coloured noise and the differences with respect to the white noise case (see Ref. [39] for a complete discussion on the effects induced by the white noise). We note that in Figs. 4, 5 the 1st order moments undergo correlated oscillations and this behaviour is independent on the correlation time (see panels (a), (b), (c)). Conversely, the presence of coloured noise affects the dynamics of the 2nd order moments, reducing the effects of the random fluctuations respect to the white noise case. In panels (e)–(i) of the same figures, we note that the amplitude of the oscillations of the 2nd order moments of the two prey densities reaches its highest value after a time interval whose length increases as τ_c becomes bigger. In panels (a)–(f) of Figs. 4, 5, the time series of mean values and variances of the two prey densities overlap and those of species x (blue line) are not visible. In panels (g)–(i) of the same figures, the covariances μ_{101} and μ_{011} overlap, being μ_{101} (red line) not visible.

3. Coupled map lattice model

In this section we use a different method to study the time evolution of the three interacting species on the spatial domain defined in Section 2. We analyse the system dynamics by using a coupled map lattice (CML) model [40]

$$\begin{aligned} x_{i,j}^{(n+1)} &= \lambda x_{i,j}^{(n)} \left(1 - \nu x_{i,j}^{(n)} - \beta^{(n)} y_{i,j}^{(n)} - \alpha z_{i,j}^{(n)}\right) + x_{i,j}^{(n)} \zeta_{i,j}^{x(n)} \\ &\quad + D \sum_{\rho} \left(x_{\rho}^{(n)} - x_{i,j}^{(n)}\right) , \qquad (29) \\ y_{i,j}^{(n+1)} &= \lambda y_{i,j}^{(n)} \left(1 - \nu y_{i,j}^{(n)} - \beta^{(n)} x_{i,j}^{(n)} - \alpha z_{i,j}^{(n)}\right) + y_{i,j}^{(n)} \zeta_{i,j}^{y(n)} \\ &\quad + D \sum_{\rho} \left(y_{\rho}^{(n)} - y_{i,j}^{(n)}\right) , \qquad (30) \\ z_{i,j}^{(n+1)} &= \lambda_z z_{i,j}^{(n)} \left(-1 + \gamma x_{i,j}^{(n)} + \gamma y_{i,j}^{(n)}\right) + \xi_{i,j}^{z(n)} \zeta_{i,j}^{z(n)} \\ &\quad + D \sum_{\rho} \left(z_{\rho}^{(n)} - z_{i,j}^{(n)}\right) , \qquad (31) \end{aligned}$$

which represents a time discrete version of the Lotka–Volterra equations. The results obtained by the two different methods, *i.e.* formalism of the moments and CML model, are compared in section 4 in view of using them to reproduce some properties of real ecosystems. Here $x_{i,j}^{(n)}$, $y_{i,j}^{(n)}$ and $z_{i,j}^{(n)}$

denote respectively the densities of prey x, prey y and predator z in the site (i,j) at the time step n. According to the notation used for the mean field approach, λ, λ_z, ν, β, α, γ and D represent the same quantities defined in Section 2. The interaction parameter $\beta^{(n)}$ corresponds to the value of $\beta(t)$ taken at the time step n, according to Eq. (12). $\zeta^{x(n)}_{i,j}$, $\zeta^{y(n)}_{i,j}$ and $\zeta^{z(n)}_{i,j}$ are the Gaussian coloured noise sources defined in Eq. (4). Here, $\sum_\rho$ indicates the sum over the four nearest neighbours.

Using this CML model, both correlated and anticorrelated spatial patterns of three interacting species have been found [41]. In this work, we obtain from Eqs. (29)–(31) the time evolution of the three species concentrations and calculate, at each time step, the corresponding mean values (1st order moments), variances and covariances (2nd order central moments).

3.1. Stationary states of the CML model

In the absence both of noise sources and diffusion terms ($D = 0$), by setting $x^{(n+1)}_{i,j} = x^{(n)}_{i,j}$, $y^{(n+1)}_{i,j} = y^{(n)}_{i,j}$, $z^{(n+1)}_{i,j} = z^{(n)}_{i,j}$, from Eqs. (29)–(31) we obtain

$$x^{\rm stat}_{\rm CML} = y^{\rm stat}_{\rm CML} = \frac{1}{2\gamma}\left[\frac{\lambda_z+1}{\lambda_z}\right], \tag{32}$$

$$z^{\rm stat}_{\rm CML} = \frac{2\gamma\left[\frac{\lambda-1}{\lambda}\right]-(\beta+\nu)\left[\frac{\lambda_z+1}{\lambda_z}\right]}{2\alpha\gamma}, \tag{33}$$

where the indices i,j were suppressed. In agreement with Eq. (9), we note that, also in the CML model, the stationary values of the two prey densities do not depend on the interaction parameter β. By using the existence condition for the predator

$$z^{\rm stat}_{\rm CML} = \frac{2\gamma\left[\frac{\lambda-1}{\lambda}\right]-(\beta+\nu)\left[\frac{\lambda_z+1}{\lambda_z}\right]}{2\alpha\gamma} > 0\,, \tag{34}$$

we get

$$\beta < 2\gamma\frac{\left[\frac{\lambda-1}{\lambda}\right]}{\left[\frac{\lambda_z+1}{\lambda_z}\right]} - \nu\,. \tag{35}$$

According to the analysis of Section 2.1, the inequality (35) indicates that in the CML model two stationary states, corresponding to coexistence and exclusion regime, are present. We note that the coexistence condition (35) depends also on the scale factors λ and λ_z (see discussion in Ref. [39]).

3.2. Time series in the CML model

To evaluate the 1st and 2nd order moments we define on the lattice, at the time step n, the mean values

$$\langle u\rangle^{(n)} = \frac{\sum_{i,j} u_{i,j}^{(n)}}{N}, \qquad (u = x, y, z), \tag{36}$$

the variances

$$\mathrm{var}_u^{(n)} = \frac{\sum_{i,j}\left(u_{i,j}^{(n)} - \langle u\rangle^{(n)}\right)^2}{N}, \qquad (u = x, y, z), \tag{37}$$

and the covariances

$$\mathrm{cov}_{uw}^{(n)} = \frac{\sum_{i,j}\left(u_{i,j}^{(n)} - \langle u\rangle^{(n)}\right)\left(w_{i,j}^{(n)} - \langle w\rangle^{(n)}\right)}{N}, \quad (u, w = x, y, z,\ u \neq w)\,. \tag{38}$$

To compare the mean field approach with the CML model, we must have $\beta = 1$ as critical value for the coexistence/exclusion regimes. Therefore, setting all parameters, except γ, at the same values of Section 2, *i.e.* $\lambda = 3$, $\lambda_z = 0.06$, $\nu = 1$, $\alpha = 0.02$, and $\gamma = 26.5$, from Eqs. (34), (35) we obtain, for $\beta < 1$, survivance of the species z and, as a consequence, coexistence of the three species. Conversely, for $\beta > 1$ exclusion regime takes place. Therefore, for $\gamma = 26.5$ a coexistence/exclusion dynamical regime is obtained, with the system driven by the same time behaviour of $\beta(t)$ used in the approach of the moments (see Eq. (12) and Fig. 2).

Finally, with these parameter values, from Eqs. (32), (33) we obtain, in coexistence regime ($\beta = \beta_{\mathrm{down}} = 0.94$), stationary values comparable with those obtained in the mean field approach (see Eqs. (28))

$$\langle x\rangle_{\mathrm{CML}}^{\mathrm{stat}} = \langle y\rangle_{\mathrm{CML}}^{\mathrm{stat}} = 0.3\,, \qquad \langle z\rangle_{\mathrm{CML}}^{\mathrm{stat}} = 1.0\,. \tag{39}$$

The CML model is based on the use of the time step $\Delta t = 1$. Conversely, Eqs. (17)–(25) have been solved by using the time step $dt = 10^{-3}$, which is a suitable value to obtain convergence of the solution. Because Δt is much larger than dt, the CML model causes the system to evolve more rapidly with respect to dynamics obtained within the formalism of the moments. To remove this discrepancy, in the discrete time equations we use a much smaller value for the diffusion constant, namely $D = 10^{-4}$ (see discussion in Ref. [39]). Here we consider a square lattice with $N = 100 \times 100$ and calculate from Eqs. (29)–(31), the time series of $x_{i,j}^{(n)}$, $y_{i,j}^{(n)}$, $z_{i,j}^{(n)}$. By this way, according to Eqs. (36)–(38), we obtain the time behaviour of the moments

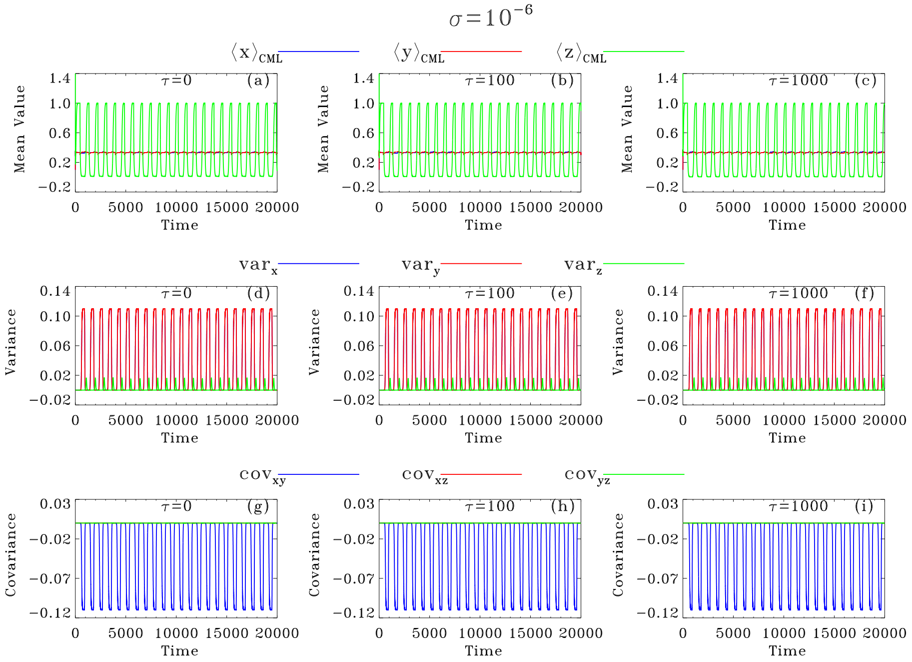

Fig. 6. Time beahviour of the mean values (panels (a), (b), (c)), variances (panels (d), (e), (f)) and covariances (panels (g), (h), (i)) of the three species concentrations, for $\sigma = 10^{-6}$ and three different values of τ_c. The time series are obtained within the formalism of the CML model. The diffusion coefficient is $D = 10^{-4}$, and $\gamma = 26.5$. The initial values of the species concentrations are $x_{i,j}^{(0)} = y_{i,j}^{(0)} = 0.1$, $z_{i,j}^{(0)} = 2.0$ for all the sites (i, j). In panels (a)–(f), the time series of mean values and variances of the two prey densities overlap ($\langle x \rangle$ and $\langle y \rangle$ maintain the constant value 0.3, while var_x and var_y oscilate between 0 and 0.11) and those of species x (blue line) are not visible. In panels (g)–(i), the covariances cov_{xz} and cov_{yz} overlap at the constant value 0.005, being cov_{xz} (red line) not visible. The values of the other parameters are the same as in Fig. 4: $\lambda = 3$, $\lambda_z = 0.06$, $\nu = 1$, $\alpha = 0.02$.

for two different values of multiplicative noise intensity and three values of correlation time. The results are shown in Figs. 6, 7. Comparing the time series of the mean values, variances and covariances obtained in the CML model with the 1st and 2nd order moments calculated within the mean field approach (see Figs. 4, 5), we note that the two set of time series are in a good qualitative agreement.

In particular, we note that, as observed in the formalism of the moments, the mean values of the three species are characterized by time oscillations, whose amplitude is larger for the predator (panels (a), (b), (c) of Figs. 6, 7). Moreover, we observe that the mean values $\langle x \rangle^{(n)}$, $\langle y \rangle^{(n)}$, $\langle z \rangle^{(n)}$ oscillate

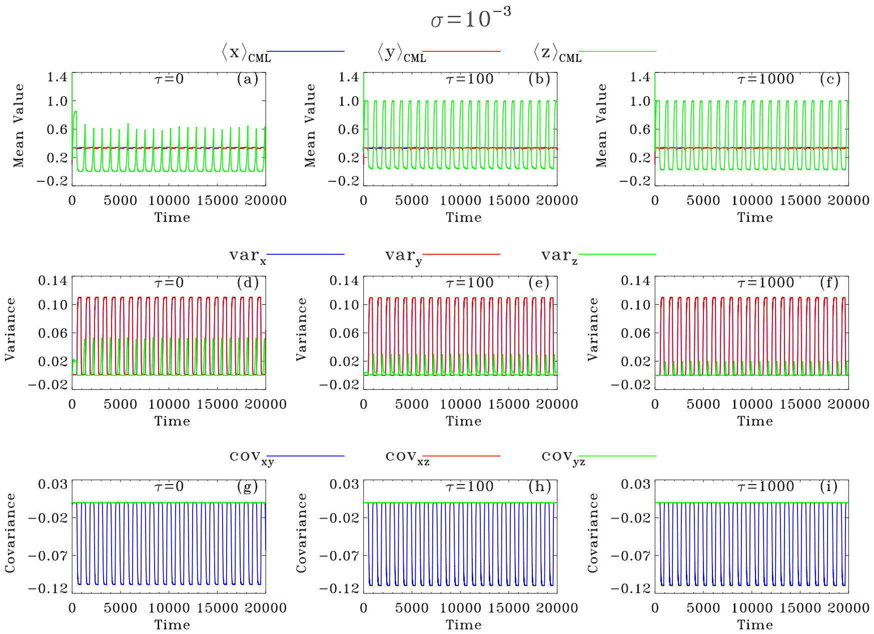

Fig. 7. Time beahviour of the mean values (panels (a), (b), (c)), variances (panels (d), (e), (f)) and covariances (panels (g), (h), (i)) of the three species concentrations, for $\sigma = 10^{-6}$ and three different values of τ_{c}. The time series are obtained within the formalism of the CML model. In panels (a)–(f), the time series of mean values and variances of the two prey densities overlap and those of species x (blue line) are not visible. In panels (g)–(i), the covariances cov_{xz} and cov_{yz} overlap, being cov_{xz} (red line) not visible. The initial conditions and parameter values are the same as in Fig. 6.

around different values with respect to $\langle x\rangle(t)$, $\langle y\rangle(t)$, $\langle z\rangle(t)$, and variances and covariances in the CML model show oscillations with significantly larger amplitude with respect to the results obtained in the mean field approach. Here, we recall the results reported in Ref. [39]: switching off the multiplicative noise sources ($\sigma = 0$), the 2nd order moments remain equal to zero, recovering the conditions of homogeneous distributions obtained for $\sigma = 0$ in the mean field approach. Introducing sources of multiplicative noise, slight modifications occur in the mean values (see panels (a), (b), (c) in Figs. 6, 7), and the system is subjected to a symmetry breaking, with non-vanishing variances that indicate inhomogeneous distributions of the three species (see panels (d), (e), (f) in Figs. 6, 7). In panels (a)–(f), the time series of mean values and variances of the two prey densities overlap and those of species x (blue line) are not visible. In panels (g)–(i) of the same figures, the covariances cov_{xz} and cov_{yz} overlap, being cov_{xz} (red line) not visible. To discuss the effects due to the coloured noise, we observe that the mean values, variances and covariances obtained in the presence of coloured noise with $\sigma = 10^{-6}$ do not show any differences with respect to the case of white noise (see Fig. 6). For a higher level of the noise intensity ($\sigma = 10^{-3}$), the amplitude of the oscillations of $\langle z \rangle_{\mathrm{CML}}$ increases for larger values of the correlation time (see panels (a), (b), (c) in Fig. 7). Moreover, the amplitude of the oscillations in the time series of var_z becomes smaller (see panels (d), (e), (f) in Fig. 7), which means that the spread out of the species z decreases, approaching the value observed in the absence of multiplicative noise. This indicates that the presence of a time correlation in the noise source tends to reduce the effects of the noise. The previous analysis shows that the presence of coloured noise produces different effects: *(i)* a delay in the time behaviour of the 2nd order moments obtained within the formalism of the moments, *(ii)* an enhancement of the oscillation amplitude of the mean value of the predator density in the CML model; *(iii)* a decrease of the oscillation amplitude of the variance of the predator density in the CML model. To explain these discrepancies in the results obtained from the two approaches we recall that: *(i)* the stationary values in the time discrete approach are different from those obtained in the moment formalism (see Eqs. (27) and Eqs. (32), (33)); *(ii)* in the mean field approach each site interacts with all other sites, conversely in the CML model the spatial interaction involves exclusively the nearest neighbours; *(iii)* in the CML model the time step is $\Delta t = 1$, while in the formalism of the moments the time step is set at $dt = 10^{-3}$.

4. Conclusions

We present the results of a study on the stochastic dynamics of three interacting species, namely two preys and one predator, distributed in a two-dimensional lattice. The system is described by generalized Lotka–Volterra equations in the presence of multiplicative coloured noise with correlation time τ_{c}, and diffusive terms with diffusion coefficient D. Moreover, the interaction parameter between the two preys, $\beta(t)$, is a stochastic process driven by a dichotomous noise, which is responsible for the dynamical regime (coexistence or exclusion) of the ecosystem. We find that the 1st order moments of the three species concentrations undergo oscillations whose amplitude does not depend on the multiplicative coloured noise. On the other side, in the 2nd order moments the multiplicative coloured noise induces oscillations whose amplitude is strongly dependent on the noise intensity. In particular, the two preys show an anticorrelated behaviour, while the predator results to be correlated with the total concentrations of the two preys. The effects of the coloured noise is to introduce a delay in the transient dynamics of the 2nd order moments: the maximum amplitude of the oscillations in the time series of variances and covariances of the prey densities is reached after a time interval that increases as τ_{c} becomes larger.

Finally, we compare the results obtained within the moment formalism with those calculated by a coupled map lattice (CML) model. In particular, we find that in the mean field approach the amplitude of the oscillations of the 2nd order moments of the two prey densities reaches its highest value after a time interval whose length increases as τ_c becomes larger. This indicates that the time correlation of the multiplicative noise delays the anticorrelated behaviour of the two preys and, as a consequence, their dispersal in the spatial domain. In a real ecosystem, characterized by a dynamical regime where coexistence and exclusion appears alternatively, these results account for the uncorrelated behaviour of two competing species which can coexist, even if exclusion takes place. In fact, in the presence of delayed noise effects, the symmetry which initially characterizes the dynamics of the two species is conserved and the two preys undergo neither dispersal nor anticorrelation in the spatial domain. Conversely, in the CML model this delay effect does not appear. Here, for suitably high values of the multiplicative noise intensity, the time correlation of the noise is responsible for an enhancement of the oscillation amplitude in the time series of $\langle z\rangle^{(n)}$ (mean value of the predator density) and a reduction of $\mathrm{var}_z^{(n)}$ (variance of the predator density). This results disagree with those obtained in the moment formalism and indicate that in the CML model the time correlation in the multiplicative noise affects the dynamics of the predator without causing any change in that of the two preys. This remarkable discrepancy with the mean field approach suggests that the dynamics of biological species in a real ecosystem can be better modelled by the formalism of the moments, which accounts for the anticorrelated behaviour observed in real populations [44,45].

We also recall that the time series of populations in real ecosystems are noisy and specifically they can be "red", that is they are dominated by low-frequency, long term variations, or white, that is they present no prevailing frequency [46–48]. In particular, "terrestrial populations exist in a white noise atmosphere, whereas marine populations are embedded in a red noise environment" (see Ref. [49]). Moreover, in the presence of red and blue environmental noise, time series of populations in real ecosystems show, respectively, more red or blue spectra than those subjected to white noise [50]. According to these findings, many ecologists have extensively accepted that environmental noises can be described by auto-correlated stochastic processes [51]. These experimental and theoretical studies indicate that a realistic choice is to use coloured noise sources in modelling population dynamics. Specifically, the spatial distributions of *benthic foraminifera* in marine environment [44] and the time behaviour of *Listeria monocytogenes* concentration (bacterial dynamics) in a food product [12], reproduced applying stochastic models based on Lotka–Volterra equations for fixed values of the interaction parameter, could be better described modelling environmental random fluctuations by auto-correlated noise sources and, eventually, introducing a dynamical coexistence/exclusion regime. We conclude observing that the theoretical results presented in this paper could be also useful to explain the dynamics of other real ecosystems [9, 10], where both deterministic and stochastic interactions can be present [42, 43, 52–54].

Authors are grateful to Prof. Lutz Schimansky-Geier for useful discussions. Authors acknowledge the financial support by ESF (European Science Foundation) STOCHDYN network and partially by MIUR.

REFERENCES

[1] R. Benzi, A. Sutera, A. Vulpiani, *J. Phys.: Math. Gen.* **14**, L453 (1981); R. Benzi, G. Parisi, A. Sutera, A. Vulpiani, *Tellus* **34**, 10 (1982).

[2] L. Gammaitoni, P. Hänggi, P. Jung, F. Marchesoni, *Rev. Mod. Phys.* **70**, 223 (1998).

[3] R.N. Mantegna, B. Spagnolo, *Phys. Rev.* **E49**, R1792 (1994).

[4] N.V. Agudov, B. Spagnolo, *Phys. Rev.* **E64**, 035102(R) (2001); N.V. Agudov, A.A. Dubkov, B. Spagnolo, *Physica A* **325**, 144 (2003); A.A. Dubkov, N.V. Agudov, B. Spagnolo, *Phys. Rev.* **E69**, 061103 (2004); A. Fiasconaro, B. Spagnolo, *Phys. Rev.* **E80**, 041110 (2009).

[5] B. Spagnolo, A. Fiasconaro, D. Valenti, *Fluct. Noise Lett.* **3**, L177 (2003).

[6] D. Valenti, A. Fiasconaro, B. Spagnolo, *Physica A* **331**, 477 (2004); B. Spagnolo, M. Cirone, A. La Barbera, F. de Pasquale, *J. Phys.: Condens. Matter* **14**, 2247 (2002).

[7] B. Spagnolo, D. Valenti, A. Fiasconaro, *Math. Biosciences Eng.* **1**, 185 (2004).

[8] C. Zimmer, *Science* **284**, 83 (1999).

[9] O.N. Bjørnstad, B.T. Grenfell, *Science* **293**, 638 (2001).

[10] B.T. Grenfell, K. Wilson, B.F. Finkenstädt, T.N. Coulson, S. Murray, S.D. Albon, J.M. Pemberton, T.H. Clutton-Brock, M.J. Crawley, *Nature* **394**, 674 (1998).

[11] O.A. Chichigina, *Eur. Phys. J.* **B65**, 347 (2008).

[12] A. Giuffrida, D. Valenti, G. Ziino, B. Spagnolo, A. Panebianco, *Eur. Food Res. Technol.* **228**, 767 (2009); E. Korobkova, T. Emonet, J.M. Vilar, T.S. Shimizu, P. Cluzel, *Nature* **428**, 574 (2004).

[13] N. Pizzolato, D. Valenti, D. Persano Adorno, B. Spagnolo, *Cent. Eur. J. Phys.* **7**, 541 (2009); I. Roeder, M. Horn, I. Glauche, A. Hochhaus, M.C. Mueller, M. Loeffler, *Nature Medicine* **12**, 1181 (2006); Y. Brumer, F. Michor, E.I. Shakhnovich, *J. Theor. Biol.* **241**, 216 (2006); F. Michor, Y. Iwasa, M. Nowak, *Proc. Natl. Acad. Sci. USA* **103**, 14931 (2006); N.L. Komarova, D. Wodarz, *Theor. Popul. Bio.* **72**, 523 (2007); N.L. Komarova, D. Wodarz, *PLoS ONE* **2**, e990 (2007); V.P. Zhdanov, *Eur. Biophys. J.* **37**, 1329 (2008).

[14] M. Hoffmann *et al., PLoS ONE* **3**, 1 (2008); V. Kaitala, J. Ylikarjula, E. Ranta, P. Lundberg, *Proc. R. Soc. Lond.* **B264**, 943 (1997); O.J. Rano, J. Paulsson, *Dev. Cell. J.* **11**, 134 (2006); E.Y. Xu, K.A. Zawadzki, J.R. Broach, *Mol. Cell.* **23**, 219 (2006).

[15] E. Korobkova, T. Emonet, JM. Vilar, TS. Shimizu, P. Cluzel, *Nature* **428**, 574 (2004).

[16] M. Thattai, A. van Oudenaarden, *Genetics* **167**, 523 (2004).

[17] M. Samoilov, S. Plyasunov, AP. Arkin, *Proc. Natl. Acad. Sci. USA* **102**, 2310 (2005).

[18] Special section on Complex Systems, *Science* **284**, 79 (1999); J.R. Chabot, J.M. Pedraza, P. Luitel, A. van Oudenaarden, *Nature* **450**, 1249 (2007); M. Kaern, T.C. Elston, W.J. Blake, J.J. Collins, *Nature Rev. Genet.* **6**, 451 (2005); B.B. Kaufmann, A. van Oudenaarden, *Curr. Opin. Genet. Dev.* **17**, 107 (2007); N. Maheshri, E.K. O'Shea, *Annu. Rev. Biophys. Biomol. Struct.* **36**, 413 (2007).

[19] S. Ciuchi, F. de Pasquale, B. Spagnolo, *Phys. Rev.* **E53**, 706 (1996); E.M. Ozbudak, M. Thattai, I. Kurtser, A.D. Grossman, A. van Oudenaarden, *Nature Genet.* **31**, 69 (2002); M.B. Elowitz, A.J. Levine, E.D. Siggia, P.S. Swain, *Science* **297**, 1183 (2002); W.J. Blake, M. Kaern, C.R. Cantor, J.J. Collins, *Nature* **422**, 633 (2003); J.M. Raser, E.K. O'Shea, *Science* **304**, 1811 (2004); J. Paulsson, *Nature* **427**, 415 (2004); L. Cai, N. Friedman, X.S. Xie, *Nature* **440**, 358 (2006).

[20] M. Scheffer, S. Carpenter, J.A. Foley, C. Folke, B. Walker, *Nature* **413**, 591 (2001); J.R Newman *et al.*, *Nature* **441**, 840 (2006); A. Bar-Even *et al.*, *Nature Genet.* **38**, 636 (2006).

[21] A.F. Rozenfeld *et al., Phys. Lett.* **A28**, 45 (2001); J.M. Raser, E.K. O'Shea, *Science* **309**, 5743 (2005); Ying-zi Shang, *Acta Mathematicae Applicatae Sinica (English Series)* **24**, 563 (2008).

[22] J.M.G. Vilar, R.V. Solé, *Phys. Rev. Lett.* **80**, 4099 (1998); Hong-Yan Liao, Bao-Quan Ai, Lian Hu, *Braz. J. Phys.* **37**, 1125 (2007).

[23] M.C. Cross, P.C. Hohenberg, *Rev. Mod. Phys.* **65**, 851 (1993).

[24] R.V. Solé, J. Valls, *Phys. Lett.* **A166**, 123 (1992).

[25] M. Kowalik, A. Lipowski, A.L. Ferreira, *Phys. Rev.* **E66**, 066107 (2002).

[26] A.R.E. Sinclair, S. Mduma, J.S. Brashares, *Nature* **425**, 288 (2003).

[27] A. Fiasconaro, D. Valenti, B. Spagnolo, *Acta Phys. Pol. B* **35**, 1491 (2004).

[28] J. Buceta, K. Lindenberg, *Phys. Rev.* **E66**, 046202 (2002).

[29] B. Bolker, S.W. Pacala, *Theor. Popul. Biol.* **52**, 179 (1997); A. Gandhi, S. Levin, S. Orszag, *Bull. Math. Biol.* **62**, 595 (2000); J. Dushoff, *Theor. Popul. Biol.* **56**, 325 (1999).

[30] D. Valenti, L. Schimansky-Geier, X. Sailer, B. Spagnolo, *Eur. Phys. J.* **B50**, 199 (2006).

[31] V.M. Peréz García, P. Torres, G.D. Montesinos, *SIAM J. Appl. Math.* **67**, 990 (2007).

[32] P. Ilg, I.V. Karlin, H.C. Öttinger, *Phys. Rev.* **E60**, 5783 (1999).

[33] A.J. Lotka, *Proc. Nat. Acad. Sci. USA* **6**, 410 (1920).

[34] V. Volterra, *Nature* **118**, 558 (1926).

[35] C.W. Gardiner *Handbook of Stochastic Methods for Physics, Chemistry and the Natural Sciences*, Springer, Berlin 1993.

[36] A.D. Bazykin, *Nonlinear Dynamics of Interacting Populations*, World Scien. Publishing, Singapore 1998.

[37] R. Kawai, X. Sailer, L. Schimansky-Geier, C. Van den Broeck, *Phys. Rev.* **E69**, 051104 (2004).

[38] D. Valenti, L. Schimansky-Geier, X. Sailer, B. Spagnolo, M. Iacomi, *Acta Phys. Pol. B* **38**, 1961 (2007).

[39] D. Valenti, B. Spagnolo, *Cent. Eur. J. Phys.* **7**, 457 (2009).

[40] K. Kaneko, *Chaos* **2**, 279 (1992); R.V. Solé, J. Bascompte, J. Valls, *Chaos* **2**, 387 (1992); R.V. Solé, J. Bascompte, J. Valls, *J. Theor. Biol.* **159**, 469 (1992).

[41] A. Fiasconaro, D. Valenti, B. Spagnolo, *Fluct. Noise Lett.* **5**, L305 (2005).

[42] J. García Lafuente, A. García, S. Mazzola, L. Quintanilla, J. Delgado, A. Cuttitta, B. Patti, *Fisheries Oceanography* **11**, 31 (2002); A. Caruso, M. Sprovieri, A. Bonanno, R. Sprovieri, *Riv. Ital. Paleont. Strat.* **108**, 297 (2002).

[43] R. Sprovieri, E. Di Stefano, A. Incarbona, M.E. Gargano, *Palaeogeography, Palaeoclimatology, Palaeoecology* **202**, 119 (2003).

[44] D. Valenti, L. Tranchina, M. Brai, A. Caruso, C. Cosentino, B. Spagnolo, *Ecol. Model.* **213**, 449 (2008).

[45] A. Caruso, M. E. Gargano, D. Valenti, A. Fiasconaro, B. Spagnolo, *Fluct. Noise Lett.* **5**, L349 (2005).

[46] S.L. Pimm, *The Balance of Nature? Ecological Issues in the Conservation of Spaecies and Communities*, University of Chicago Press, Chicago 1991.

[47] G. Sugihara, *Nature* **378**, 559 (1995).

[48] J.M. Halley, *Trends Ecol. Evol.* **11**, 33 (1996).

[49] J.H. Steele, E.W. Henderson, *Proc. R. Soc. Lond.* **B343**, 5 (1994).

[50] V. Kaitala, J. Ylikarjula, E. Ranta, P. Lundberg *Proc. R. Soc. Lond.* **B264**, 943 (1997).

[51] M. Gao, Z. Li, H. Dai, *Ecol. Model.* **201**, 326 (2007).

[52] M. Gutiérrez, G. Swartzman, A. Bertrand, S. Bertrand, *Fisheries Oceanography* **16**, 155 (2007).

[53] S. Bertrand, E. Díaz, M. Lengaigne, *Progress in Oceanography* **79**, 379 (2008).

[54] Z. Liu, M. Gao, F. Zhanga, Z. Li, *BioSystems* **98**, 115 (2009).